Available online at www.sciencedirect.com
ScienceDirect
Journal of Hazardous Materials 149 (2007) 518–522
Journal of Hazardous Materials
www.elsevier.com/locate/jhazmat

An assessment of the role of intracellular reductive capacity in the biological clearance of triarylmethane dyes

Özden Tacal *, Inci Özer

Department of Biochemistry, School of Pharmacy, Hacettepe University, 06100 Ankara, Turkey

Received 12 June 2007; received in revised form 4 August 2007; accepted 8 August 2007
Available online 12 August 2007

Abstract

The second-order rate constants (at pH 7, 25 °C) for the reduction of three cationic triarylmethane dyes [pararosaniline (PR^+), malachite green (MG^+), methyl green (MeG^+)] by NADH were 1.4×10^{-2} to 6.7×10^{-2} mM^{-1} min^{-1}. Based on these values the intracellular nonenzymatic reduction of TAM^+ to TAM-H by endogenous NADH was estimated to proceed with an average half-life of 30 min. Rapid and significant adduct formation was observed with the thiol, 3-mercaptopropionic acid (MPA), suggesting that the primary intracellular form of the dyes must be a thiol adduct and that the conversion to adduct form takes place within ms–s. These time frames, when compared to the min–h time frame for microbial clearance of triarylmethanes from culture media, suggest that transport must be the rate-limiting step in nonadsorptive (chemical) clearance of the dyes and that the presence of enzymes to complement the nonenzymatic reductive and adduct-forming activities cited serves a kinetically limited purpose. It appears that a superior *catalytic* scavenger will be one with a superior transport capacity.

Keywords: Malachite green; Methyl green; Pararosaniline; Triarylmethane reductase; Thiol adduct

1. Introduction

Cationic triarylmethane dyes (TAM^+s) have been widely used as colorants in industry and as antimicrobial/antiparasitic agents in fish and poultry farming as well as in human medicine [1,2]. While the use of TAM^+s has been discouraged in later years in view of the toxic and mutagenic threat to human health [3–6], the dyes continue to serve both in industry and as frequent tools and reagents in analytical, cell biological and biomedical research [7–11].

The toxicity of TAM^+s derives from changes in DNA structure and membrane permeability, $TAM^\bullet$ radical-induced redox changes in cellular components and ligand effects on protein function [1,4–6,12–18]. Studies on the biodegradation of TAM^+s in laboratory animals show N-oxides, leuko-dyes and *N*-demethylated species to be major metabolites generated by the action of peroxidases and the microsomal drug metabolizing system [3,14,19,20]. Microbial metabolism involves laccases and peroxidases [21]. Recent reports suggest that specific NADH-dependent triarylmethane reductases may also contribute to the microbial transformation of the dyes [22,23]. As TAM^+ metabolites are at least as toxic as the parent compounds, their generation does not significantly alter the toxic load on exposed organisms [3–5]. Therefore, the primary objective is to reduce exposure—by restricted utilization and by measures of remediation.

Work on environmental remediation has focused on the removal of TAM^+s from industrial wastewaters by chemical or biomass-mediated means [1,21]. The latter approach hangs principally on the clarification of polluted waters by adsorption, accompanied by uptake and metabolic processing of the dyes. Various organisms have been studied with respect to their adsorptive and metabolic capacities [22–24]. Native and recombinant species with high redox enzymatic capacity are of interest as potentially superior scavengers [23]. However, the immediate contribution of metabolic conversions to scavenger performance is not yet well established. Since a number of non-metabolic processes (such as adsorption, transport and adduct formation with cellular components) also result in dye remo-

Abbreviations: MeG^+, methyl green; MG^+, malachite green; MOPS, 3-(*N*-morpholino)propanesulfonic acid; MPA, 3-mercaptopropionic acid; NADH, β-nicotinamide adenine dinucleotide; PR^+, pararosaniline; TAM, triarylmethane; $TAM^\bullet$, triarylmethane radical; TAMR, triarylmethane reductase

* Corresponding author. Fax: +90 312 4322604.
E-mail address: tacal@hacettepe.edu.tr (Ö. Tacal).

0304-3894/$ – see front matter © 2007 Elsevier B.V. All rights reserved.
doi:10.1016/j.jhazmat.2007.08.022

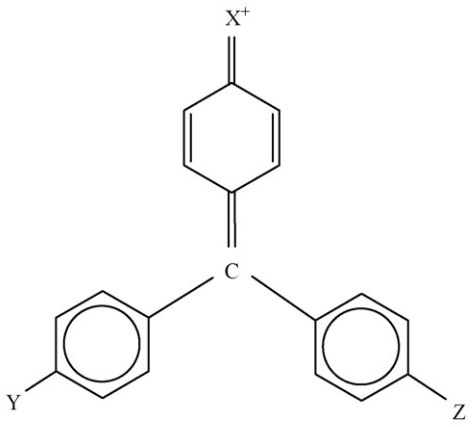

[**PR**$^+$: X = Y = Z = NH_2; **MG**$^+$: X = Y = $N(CH_3)_2$, Z = H; **MeG**$^+$: X = Y = $N(CH_3)_2$, Z = $N^+(CH_3)_2$ (CH_2CH_3)].

Fig. 1. Chemical structure of TAM^+ dyes.

val, an assessment of the relative contributions of metabolic and nonmetabolic components to the progress of biomass-mediated bleaching might be helpful in the search for suitable organisms. The present report focuses specifically on the likely role of NADH-dependent triarylmethane reductase (TAMR) activity in the environmental clearance of TAM^+s. As a first step towards evaluating reductase-mediated *versus* nonenzymatic and adsorptive processes, we have studied the nonenzymatic reactions of three TAM^+ dyes (Fig. 1) with 3-mercaptopropionic acid (MPA) and NADH. MPA was used as a model for glutathione and protein-SH groups, both of which have a pronounced tendency to form TAM–thiol adducts [25,26]. NADH was used to assess the nonenzymatic reduction potential of TAM^+s. The results are discussed with reference to information on TAM^+ reductase and the likely contribution of reductases to dye clearance [23,24].

2. Materials and methods

Malachite green (MG^+) hydrochloride, leucomalachite green, methyl green (MeG^+) zinc chloride, pararosaniline (PR^+) acetate, 3-mercaptopropionic acid and β-nicotinamide adenine dinucleotide (NADH) were purchased from Sigma–Aldrich Chemical Co., USA. Stock solutions of the dyes (5 mM, based on nominal dye content) were prepared daily in methanol. Solutions of MPA and NADH were prepared just before use in 100 mM 3-(*N*-morpholino) propanesulfonic acid (MOPS) buffer pH 7. In the case of MPA the buffer solution was supplemented with an equivalent amount of KOH to neutralize the acidic solute.

Spectrophotometric studies were performed at 25 °C using a Shimadzu 1601 PC spectrophotometer equipped with a Peltier unit. Linear regression analyses were performed using Excel©-software.

2.1. The reaction of TAM^+s with MPA and NADH

The reactions were carried out in 50 mM MOPS buffer, pH 7, containing 25 μM TAM^+ and 0–8 mM MPA or NADH. The process was initiated by the addition of dye and the bleaching was monitored spectrophotometrically at the λ_{max} of the dye being used ($l = 0.5$ cm): MG^+, 620 nm ($\varepsilon = 65\ mM^{-1}\ cm^{-1}$); MeG^+, 635 nm ($\varepsilon = 53\ mM^{-1}\ cm^{-1}$); PR^+, 540 nm ($\varepsilon = 64\ mM^{-1}\ cm^{-1}$). Each reaction was carried out in triplicate. Control experiments were conducted in the absence of MPA and NADH to estimate the basal rates and equilibria for carbinol formation. Where warranted, the data obtained with MPA and NADH were corrected for the contribution of water to the overall bleaching process (cf. Section 3).

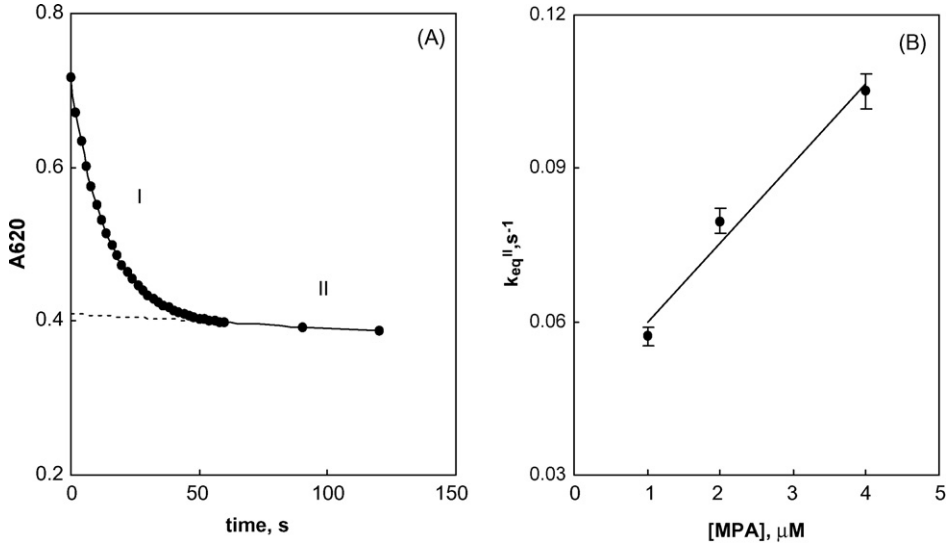

Fig. 2. The reaction of MG^+ with MPA at pH 7.0. (A) Time course for the reaction of MG^+ with MPA. [MG^+] = 25 μM; [MPA] = 2 mM. (B) Dependence of k''_{eq} for MG–MPA adduct formation on $[MPA]_T$ (the points represent mean ± S.D. values. Excel©trendline equation: $y = 0.0155x + 0.0445$; $r^2 = 0.952$).

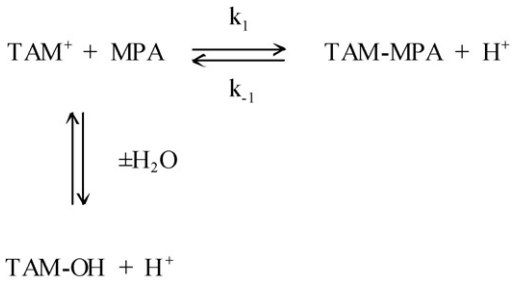

Scheme 1.

3. Results

3.1. The reaction of TAM+s with MPA

The progress curves for the bleaching of TAM+s by MPA were biphasic (Fig. 2A). As reported previously [25], the curves were analyzed according to Scheme 1, which relates the rapidly progressing phase I to the equilibration of TAM+ and TAM–MPA adduct and phase II to the gradual, solvolytic displacement towards TAM-OH. The contribution of the solvolytic process to observed bleaching in phase I was negligible, as judged by the shape of the progress curves and supported by rate constants relating to carbinol and TAM–MPA adduct formation (cf. Table 1): the estimated abundances of PR-OH, MG-OH and MeG-OH at the end of phase I are 1.8%, 0.63% and 0.06%, respectively.

The apparent rate and equilibrium constants at pH 7 for the TAM+ ⇔ TAM–MPA interconversion (k'_1, k'_{-1} and $K'_d = k'_{-1}/k'_1$) were obtained by analysis of the progress curves as follows: the reactions were conducted under pseudofirst-order conditions with [H+] constant; [nucleophile]$_T \gg$ [TAM+]$_T$. The rate constant for the initial approach to equilibrium at pH 7 (k''_{eq}, phase I) was obtained by using Eq. (1). [A_o, overall absorbance at $t = 0$; A_t, overall absorbance at $t = t$; $A_{ii,o}$, extrapolated contribution of phase II to zero time absorbance; $A_{ii,t}$ extrapolated contribution of phase II to overall absorbance at time t; $C = \ln(A_o - A_{ii,o})$]. The individual rate constants for the forward and reverse reactions (k'_1 and k'_{-1}) and K'_d were then estimated with reference to Eq. (2), which relates to pseudofirst-order reversible processes (K_a, dissociation constant of the thiol group of MPA). Plots of k''_{eq} *versus* [MPA]$_T$ yielded $k'_1 = k_1\{K_a/(K_a + [H^+])\}$ and $k'_{-1} = k_{-1}$ [H+] (Fig. 2B)

$$\ln(A_t - A_{ii,t}) = C - k''_{eq}t \quad (1)$$

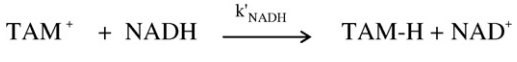

Scheme 2.

$$k''_{eq} = k_1\left\{\frac{K_a}{K_a + [H^+]}\right\}[MPA]_T + k_{-1}[H^+] \quad (2)$$

The rate and equilibrium constants for TAM–MPA adduct formation are shown in Table 1.

3.2. The reaction of TAM+s with NADH

The reduction of TAM+s by NADH was treated as an irreversible process (Scheme 2).

(The reactions were kinetically complicated by the long-term instability of NADH, such that reliable equilibrium measurements were not possible. Under second-order conditions ([NADH]$_o \approx$ [TAM+]$_o$), reduction was slow and the system was subject to error from the baseline decomposition of the cofactor; at higher NADH concentrations, residual [TAM+] (if any) was too low to measure. The absence of a significant reverse reaction has been inferred from (a) available redox potentials ($E^{o\prime}$, NAD+ = −0.320 V [27]; $E^{o\prime}$, MG+ = +0.489 V [28]), (b) the observed nonreactivity of NAD+ with leucomalachite green and (c) the insensitivity of the kinetic course of TAM+ reduction to excess added NAD+). The reductive process was monitored under pseudofirst-order conditions ([NADH]$_o \gg$ [TAM+]$_o$). The concentration of NADH was varied between limits (0.9–0.7 mM) where the reaction with TAM+s proceeded 10^2 to 10^3 times faster than the basal degradation of NADH in the buffer medium (the half-life of NADH in 100 mM MOPS (pH 7) as judged by the decrease in absorbance at 340 nm = > 40 h. The half lives for NADH-mediated bleaching of TAM+s were 3–40 min). The progress curves were analyzed as above, using the relationship $\ln(A_t - A_\infty) = C - k''_{NADH}t$, where $k''_{NADH} = k'_{NADH}$[NADH]$_o$. The second-order rate constant, k'_{NADH} (at pH 7) was obtained from replots of k''_{NADH} *versus* [NADH]$_o$. Typical data are presented in Fig. 3. The results are given in Table 1.

4. Discussion

Overall, the trends in K'_d, k'_1 and k'_{NADH} for the reactions of the dyes with MPA and NADH reflected the electrophilic character of the TAM+ nucleus as measured by affinity for water as a nucleophile (Table 1 and [29]): thus there was a positive correlation between the equilibrium constants for the formation

Table 1
Rate and equilibrium constants for the reaction of TAM+ dyes with water, MPA and NADH at pH 7, 25°

Dye	Reaction with water			Reaction with MPA			Reaction with NADH
	k'_1 $x10^7$ (mM^{-1} min^{-1})	k'_{-1} (min^{-1})	$K_d \times 10^{-3}$ (mM)	k'_1 (mM^{-1} min^{-1})	k'_{-1} (min^{-1})	K_d (mM)	$k'_1 x10^2$ (mM^{-1} min^{-1})
PR+	3.4 ± 0.45	0.099 ± 0.013	290 ± 38	0.62 ± 0.10	5.9 ± 0.60	9.5 ± 1.8	1.9 ± 0.07
MG+	2.1 ± 0.05	0.011 ± 0.0003	55 ± 0.06	0.93 ± 0.09	2.7 ± 0.13	2.9 ± 0.45	1.2 ± 0.17
MeG+	1.9 ± 0.45	0.0013 ± 0.0003	6.8 ± 1.6	19 ± 4.0	1.9 ± 0.65	0.10 ± 0.06	6.7 ± 0.94

Data are expressed as mean ± S.D.

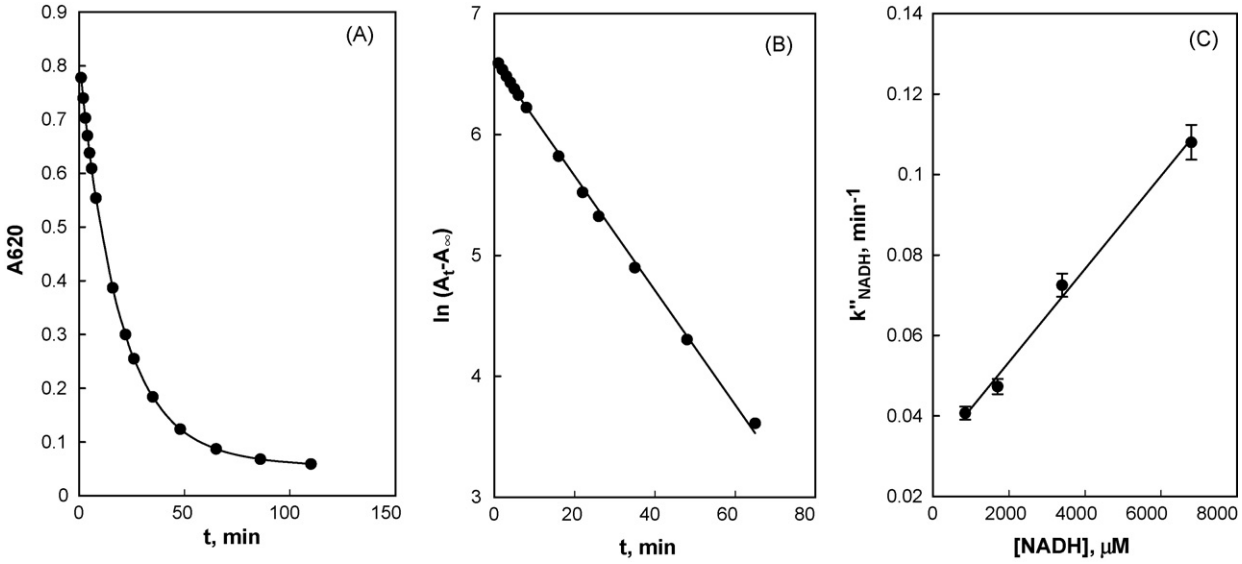

Fig. 3. The reaction of MG^+ with NADH at pH 7. (A) Time course for the reaction of MG^+ with NADH [MG^+] = 25 μM; [NADH] = 1.7 mM. (B) Semilogarithmic plot of the change in MG^+ absorbance as a function of time. (C) Dependence of k''_{NADH} on $[NADH]_T$ (the points represent mean ± S.D. values. Excel©trendline equation: $y = 0.000012x + 0.030287$; $r^2 = 0.994$).

of TAM–water adducts ($1/K_d$ or pK_d) and the corresponding constants for the formation of TAM–MPA adducts; a similar correlation was observed between the rate constants for thiol addition or hydride transfer from NADH and the affinity of the TAM^+ nucleus for water. Some of these correlations are depicted in Fig. 4.

The formation of the thiol adduct was a kinetically and thermodynamically favorable process. Considering the intracellular

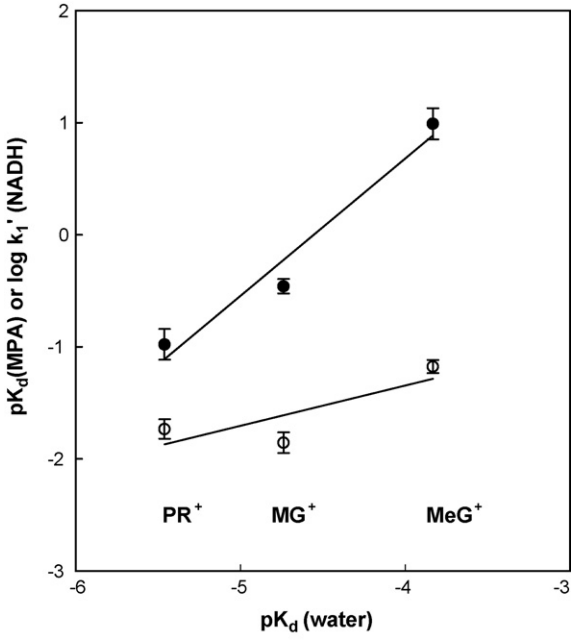

Fig. 4. Rate and equilibrium constant correlations in the reactions of TAM^+ dyes with water, MPA and NADH: (●), relationship between the equilibrium constants for water and MPA adduct formation (trendline slope = 1.23; $r^2 = 0.959$); (◯), relationship between water adduct formation and the rate of hydride transfer from NADH (trendline slope = 0.359; $r^2 = 0.655$). The points correspond to (from left to right) PR^+, MG^+ and MeG^+.

levels of glutathione and protein-SH (reported to total ca. 40 mM [30]) and the rate and equilibrium constants in Table 1, it follows that the principal intracellular form of the dyes studied must be a thiol adduct (ca. 80% of PR^+ and >99% of MeG^+) and that the conversion to adduct form takes place within a ms–s time frame.

The reduction of the dyes by NADH, while 30–300-fold slower than the reactions with MPA, still proceeded at a significant rate. Taking intracellular [NADH] ≈ 0.80 mM (in *E. coli* and yeast [31,32]), and average $k'_1 = 2.9 \times 10^{-2}\ mM^{-1}\ min^{-1}$ (Table 1), the basal pseudofirst-order rate constant for TAM^+ reduction (k''_{NADH}) is estimated to be $0.023\ min^{-1}$. Thus, endogenous NADH is expected to reduce TAM^+ to TAM-H with a half-life ($t_{0.5}$) of 30 min at 25 °C, pH 7.

The existence of TAM^+ reductase activity can theoretically reduce the residence time of the dye cations by several orders of magnitude. The data on TAMR in *Citrobacter* sp. indicates that this organism may be capable of such catalysis [23]: the estimated intracellular catalytic potential is ca. 100 units/ml or 100 mM dye reduced/min (based on a cellular protein content of 15% (w/w) and the reported enzyme specific activity of 0.5 unit/mg protein in crude homogenates). On the other hand, in culture media with cell densities of ca. 0.5 mg/ml (equivalent to 0.08 mg protein/ml, hence a TAMR capacity 40 μM/min), the clearance of experimental levels of dye (50–100 μM) is found to span several hours [33]. This implies that the decolorization process must be limited by the rate of cellular uptake, rather than the rates of subsequent reactions. If such is the case, the intracellular enzymatic arsenal is unlikely to make an immediate contribution to the NADH-coupled clearance of TAM^+s from the extracellular environment.

5. Conclusions

With transport as the rate-limiting step, the presence of a reductase to complement the nonenzymatic reductive and

adduct-forming activities cited described in this study can serve only a long-term purpose, e.g. the conversion of the dyes to insoluble or nontransportable forms. It appears, therefore, that a superior *catalytic* scavenger (as distinguished from an adsorbant) will be one with a superior transport capacity.

Acknowledgement

This study has been supported by a grant (SBAG-2912) from the Scientific and Technical Research Council of Turkey.

References

[1] D.F. Duxbury, The photochemistry and photophysics of triphenylmethane dyes in solid and liquid media, Chem. Rev. 93 (1993) 381–433.
[2] R. Docampo, R.P.A. Muniz, F.S. Cruz, R.P. Mason, Light-enhanced free radical formation and trypanocidal action of gentian violet, Science 220 (1983) 1292–1295.
[3] S.J. Culp, L.R. Blankenship, D.F. Kusewitt, D.R. Doerge, L.T. Mulligan, F.A. Beland, Toxicity and metabolism of malachite green and leucomalachite green during short-term feeding to Fischer 344 rats and B6C3F1 mice, Chem. Biol. Interact. 122 (1999) 153–170.
[4] S.J. Culp, F.A. Beland, R.H. Heflich, R.W. Benson, L.R. Blankenship, P.J. Webb, P.W. Mellick, R.W. Trotter, S.D. Shelton, K.J. Greenlees, M.G. Manjanatha, Mutagenicity and carcinogenicity in relation to DNA adduct formation in rats fed leukomalachite gren, Mutat. Res. 506/507 (2002) 55–63.
[5] S. Srivastava, R. Sinha, D. Roy, Toxicological effects of malachite green, Aquat. Toxicol. 66 (2004) 319–329.
[6] H. Ashra, K.K. Rao, Elevated phosphorylation of Chk1 and decreased phosphorylation of Chk2 are associated with abrogation of G2/M checkpoint control during transformation of Syrian hamster embryo (SHE) cells by malachite green, Cancer Lett. 237 (2006) 188–198.
[7] R. Lichtinghagen, Determination of Pulmozyme® (dornase alpha) stability using a kinetic colorimetric DNase I activity assay, Eur. J. Pharm. Biopharm. 63 (2006) 365–368.
[8] M.N. Stojanovic, D.M. Kolpashchikov, Modular aptameric sensors, J. Am. Chem. Soc. 126 (2004) 9266–9270.
[9] D.G. Jay, T. Sakurai, Chromophore assisted laser inactivation (CALI) to elucidate cellular mechanisms of cancer, Biochim. Biophys. Acta 1424 (1999) M39–M48.
[10] I.K. Kandela, J.A. Bartlett, G.L. Indig, Effect of molecular structure on the selective phototoxicity of triarylmethane dyes towards tumor cells, Photochem. Photobiol. Sci. 1 (2002) 309–314.
[11] T. Yogo, K. Kikuchi, T. Inoue, K. Hirose, M. Iino, T. Nagano, Modification of intracellular Ca^{2+} dynamics by laser inactivation of inositol 1,4,5-trisphosphate receptor using membrane-permeant probes, Chem. Biol. 11 (2004) 1053–1058.
[12] F.R. Gadelha, S.N.J. Moreno, W. De Souza, F.S. Cruz, R. Docampo, The mitochondrion of *Trypanosoma cruzi* is a target of crystal violet toxicity, Mol. Biochem. Parasitol. 34 (1989) 117–126.
[13] A.J. Kowaltowski, J. Turin, G.L. Indig, A.E. Vercesi, Mitochondrial effects of triarylmethane dyes, J. Bioenerg. Biomembr. 31 (1999) 581–590.
[14] F.E. Beyhl, Interaction of organic dyes with hepatic microsomal drug-metabolizing monooxygenases in vitro, Experientia 37 (1981) 943–945.
[15] D.A. Bullough, E.A. Cerracelli, D. Roise, W.S. Allison, Inhibition of mitochondrial F_1-ATPase by cationic dyes and amphipathic peptides, Biochim. Biophys. Acta 975 (1989) 377–383.
[16] P. Debnam, S. Glanville, A.G. Clark, Inhibition of glutathione S-transferases from rat liver by basic triphenylmethane dyes, Biochem. Pharmacol. 45 (1993) 1227–1233.
[17] M.M. Lurtz, S.E. Pedersen, Aminotriarylmethane dyes are high-affinity noncompetitive antagonists of the nicotinic acetylcholine receptor, Mol. Pharmacol. 55 (1999) 159–167.
[18] T. Küçükkilinç, I. Özer, Inhibition of human plasma cholinesterase by malachite green and related triarylmethane dyes: mechanistic implications, Arch. Biochem. Biophys. 440 (2005) 118–122.
[19] D.R. Doerge, H.C. Chang, R.L. Divi, M.I. Churchwell, Mechanism for inhibition of thyroid peroxidase by leukomalachite green, Chem. Res. Toxicol. 11 (1998) 1098–1104.
[20] W.G. Harrelson Jr., R.P. Mason, Microsomal reduction of gentian violet, Mol. Pharmacol. 22 (1982) 239–242.
[21] W. Azmi, R.K. Sani, U.C. Banerjee, Biodegradation of triphenylmethane dyes, Enzyme Microb. Technol. 22 (1998) 185–191.
[22] F. Yuzhu, T. Viraraghavan, Fungal decolorization of dye waste waters: a review, Bioresour. Technol. 79 (2001) 251–262.
[23] M.S. Jang, Y.M. Lee, C.H. Kim, J.H. Lee, D.W. Kang, S.J. Kim, Y.C. Lee, Triphenylmethane reductase from *Citrobacter* sp. Strain KCTC 18061P: purification, characterization, gene cloning and overexpression of a functional protein in *Escherichia coli*, Appl. Environ. Microbiol. 71 (2005) 7955–7960.
[24] J.P. Jadhav, S.P. Govindwar, Biotransformation of malachite green by *Saccharomyces cerevisiae* MTCC 463, Yeast 23 (2006) 315–323.
[25] Y. Eldem, I. Özer, Electrophilic reactivity of cationic triarylmethane dyes towards proteins and protein-related nucleophiles, Dyes Pigm. 60 (2004) 49–54.
[26] Ö. Tacal, I. Özer, Adduct forming tendencies of cationic triarylmethane dyes with proteins: metabolic and toxicological implications, J. Biochem. Mol. Toxicol. 18 (2004) 253–256.
[27] K.J. Laidler, Physical Chemistry with Biological Applications, Benjamin/Cummings, California, 1978, p. 356.
[28] X. Hu, K. Jiao, W. Sun, J.Y. You, Electrochemical and spectroscopic studies on the interaction of malachite green with DNA and its application, Electroanalysis 18 (2006) 613–620.
[29] S.K.S. Gupta, S. Mishra, R. Rani, A study on equilibrium and kinetics of carbocation-to-carbinol conversion for di- and triarylmethane dye cations in aqueous solutions: relative stabilities of dye carbocations and mechanism of dye carbinol formation, Indian J. Chem. 39A (2000) 703–708.
[30] F. Rusnak, T. Reiter, Sensing electrons: protein phosphatase redox regulation, Trends Biochem. Sci. 25 (2000) 527–529.
[31] J.L. Brumaghim, Y. Li, E. Henle, S. Linn, Effects of hydrogen peroxide upon nicotinamide nucleotide metabolism in *E. coli*, J. Biol. Chem. 278 (2003) 42495–42504.
[32] S.J. Lin, E. Ford, M. Haigis, G. Liszt, L. Guarante, Calorie restriction extends yeast life span by lowering the level of NADH, Genes Dev. 18 (2004) 12–16.
[33] S.Y. An, S.K. Min, I.H. Cha, Y.L. Choi, Y.S. Cho, C.H. Kim, Y.C. Lee, Decolorization of triphenylmethane and azo dyes by *Citrobacter* sp., Biotechnol. Lett. 24 (2002) 1037–1040.